· Article · Advances in Polar Science
doi: 10.12429/j.advps.2024.0001 June 2024 Vol. 35 No. 2: 192-205

Polymetamorphism of the ultrahigh-temperature granulites in the Rauer Group, East Antarctica: new evidence from zircon SHRIMP U-Pb ages

TONG Laixi[1*], LIU Zhao[1], LI Chao[1], LU Junsheng[1], YANG Wenqiang[1] & WANG Yanbin[2]

[1] State Key Laboratory of Continental Dynamics, Department of Geology, Northwest University, Xi'an 710069, China;
[2] Institute of Geology, Chinese Academy of Geological Sciences, Bejing 100037, China

Received 8 January 2024; accepted 3 June 2024; published online 30 June 2024

Abstract The Rauer Group is located on the eastern margin of the early Paleozoic Prydz Belt in East Antarctica, and the typical ultrahigh-temperature (UHT, >900 ℃) granulites outcrop on Mather Peninsula. However, the timing of UHT metamorphism and P–T path of the UHT granulites have long been debated, which is critical to understanding the tectonic nature and evolution history of the Prydz Belt. Thus, both a sapphirine-bearing UHT metapelitic granulite and a garnet-bearing UHT mafic granulite are selected for zircon SHRIMP U-Pb age dating. The results show that metamorphic zircon mantles yield weighted mean $^{206}Pb/^{238}U$ ages of 918±29 Ma and 901±29 Ma for the metapelitic and mafic granulites, respectively, while zircon rims and newly grown zircons yield weighted mean $^{206}Pb/^{238}U$ ages of 523±9 Ma and 532±11 Ma, respectively. These new zircon age data suggest that the UHT granulites may have experienced polymetamorphism, in which pre-peak prograde stage occurred in the early Neoproterozoic Grenvillian orogenesis (1000–900 Ma), whereas the UHT metamorphism occurred in the late Neoproterozoic to early Paleozoic Pan-African orogenesis (580–460 Ma). This implies that P–T path of the UHT granulites should consist of two separate high-grade metamorphic events including the Grenvillian and Pan-African events, which are supposed to be related to assembly of Rodinia and Gondwana supercontinents respectively, and hence the overprinting UHT metamorphic event may actually reflect an important intracontinental reworking.

Keywords **ultrahigh-temperature granulites**, **zircon SHRIMP U-Pb ages**, **polymetamorphism**, **Rauer Group**, **East Antarctica**

Citation: Tong L X, Liu Z, Li C, et al. Polymetamorphism of the ultrahigh-temperature granulites in the Rauer Group, East Antarctica: new evidence from zircon SHRIMP U-Pb ages. Adv Polar Sci, 2024, 35(2): 192-205, doi: 10.12429/j.advps.2024.0001

1 Introduction

The sapphirine-bearing ultrahigh-temperature (UHT, >900 ℃) granulites occur on Mather Peninsula in the Rauer Group (Harley, 1998; Harley and Fitzsimons, 1991; Kelsey et al., 2007; Liu et al., 2023; Tong and Wilson, 2006), which is located on the eastern margin of the early Paleozoic Prydz Belt in East Antarctica (Figure 1). Since the Prydz Belt was recognized as an extensive Pan-African (550–500 Ma) high-grade tectonic mobile belt in East Antarctica (Carson et al., 1996; Dirks and Wilson, 1995; Fitzsimons, 1997; Hensen and Zhou, 1995; Zhao et al., 1995), extending along the Prydz Bay coast from the Rauer Group in the east to the Larsemann Hills and the Amery area in the west, and then further to the inland Grove Mountains (Liu et al., 2002, 2006, 2007, 2009a, 2018; Zhao et al., 2003). This led to two contrasting points of view on the tectonic nature of the

* Corresponding author, ORCID: 0000-0002-4416-9583, E-mail: tonglx@nwu.edu.cn

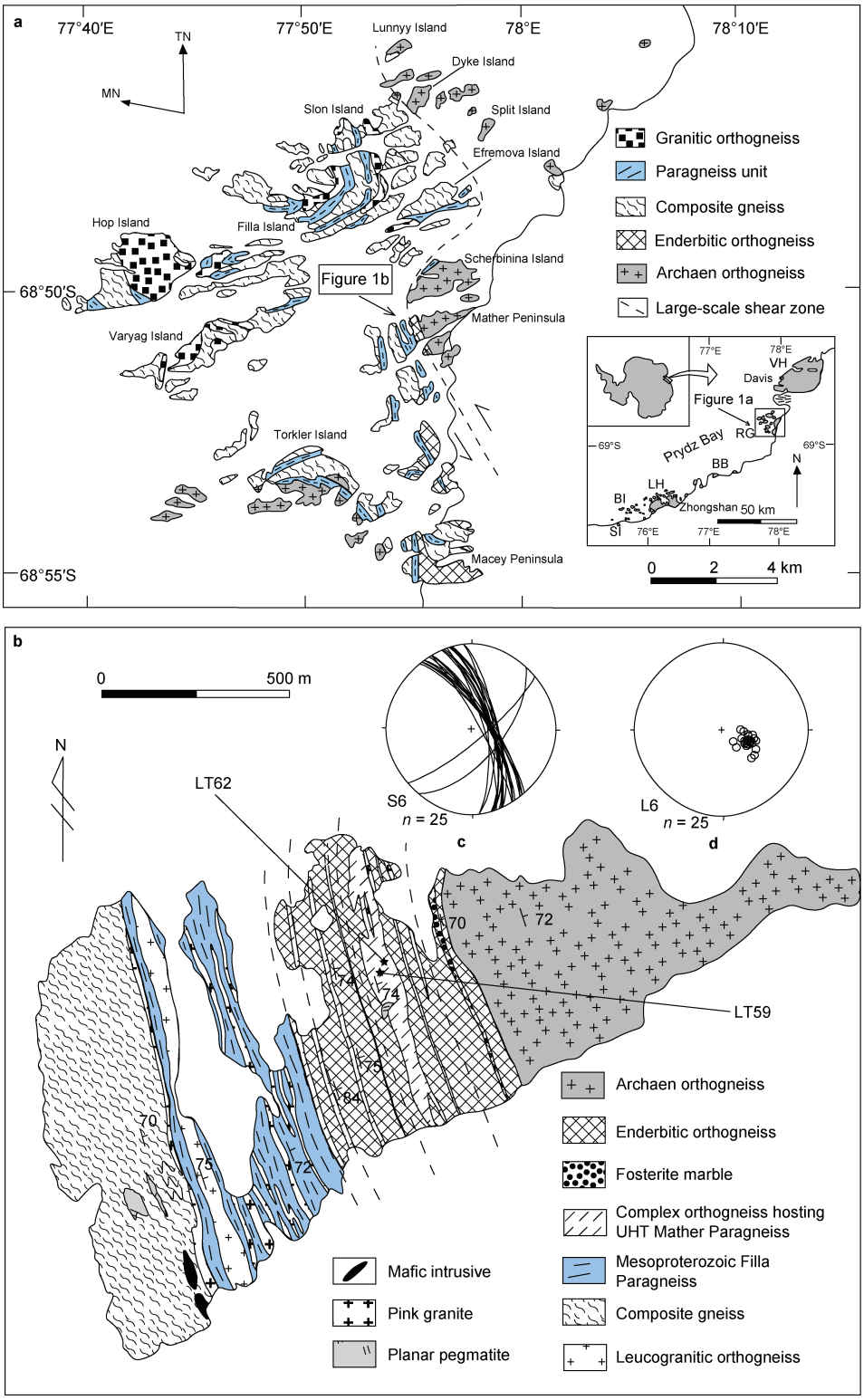

Figure 1 Geological maps of the Rauer Group and Mather Peninsula (after Tong and Wilson, 2006). **a**, geological map of the Rauer Group. Insert shows the locations of the Rauer Group (RG), Vestfold Hills (VH), Brattstran Bluffs (BB), Larsemann Hills (LH), Søstrene Island (SI) and Bolingen Islands (BI), the dashed line shows the major Mather Shear Zone defined by a ~500 m wide planar high-strain zone; **b**, lithological distribution and sample locations on Mather Peninsula, the dashed lines show representative recognized cm- to m-wide high-grade shear zones; **c** and **d** show stereographic projections for the major foliation orientations and mineral elongation lineations on Mather Peninsula. LT59 and LT62 indicate two analyzed samples in this study; L6 indicates stretching lineation related to D6 deformation; S6 indicates gneissic foliation associated with D6 deformation.

Prydz Belt: (1) The rocks experienced a single Pan-African high-grade tectonothermal event (Carson et al., 1997; Chen et al., 2023; Fitzsimons, 1996; Liu et al., 2006, 2007; Wang et al., 2022), and the belt was considered to represent an early Paleozoic suture zone or orogen associated with the final assembly of Gondwana supercontinent (Boger, 2011; Boger et al., 2001; Fitzsimons, 2000; Harley et al., 2013; Hensen and Zhou, 1997; Liu et al., 2007, 2009a); (2) The rocks underwent two phases of metamorphism and the P–T path was thought to consist of two high-grade structural-metamorphic events, namely the early Neoproterozoic Grenvillian (990–900 Ma) and the early Paleozoic Pan-African (550–500 Ma) (Dirks and Hand, 1995; Dirks et al., 1994; Grew et al., 2012; Liu et al., 2013; Spreitzer et al., 2021; Tong and Wilson, 2006; Tong et al., 2002, 2014, 2019), or two high-grade metamorphic events at ~800 Ma and ~500 Ma (Arora et al., 2020), while the latter should represent an intracontinental reworking event (Harley, 2014; Phillips et al., 2007; Ren et al., 2016, 2018; Tong et al., 2014, 2017; Wilson et al., 2007), and hence the Prydz Belt should belong to a polymetamorphic terrain (Dirks and Wilson, 1995; Liu, 2009; Liu et al., 2009b; Thost et al., 1991; Tong et al., 2019).

As an important part of the Prydz Belt, since the sapphirine-bearing UHT granulites have firstly been reported from the Rauer Group (Harley and Fitzsimons, 1991), up to recently, the timing of UHT metamorphism and P–T path of the UHT granulites are still debated (Chen et al., 2023; Clark et al., 2019; Harley, 1998; Hokada et al., 2016; Kelsey et al., 2007; Liu et al., 2023; Tong and Wilson, 2006; Wang et al., 2007). For instance, the UHT metamorphism was considered to occur in the early Neoproterozoic (1000–900 Ma) (Tong and Wilson, 2006; Wang et al., 2007; Wu et al., 2023), or in the early Paleozoic (550–500 Ma) (Chen et al., 2023; Clark et al., 2019; Kelsey et al., 2007; Liu et al., 2021; Sims and Wilson, 1997), or in the late Neoproterozoic (Harley, 2014; Harley et al., 2009; Hokada et al., 2016; Liu et al., 2023). On the other hand, distinct-type P–T paths of pre-peak and post-peak evolution histories for the UHT granulites were also inferred by different researchers (Figure 2) (Chen et al., 2023; Clark et al., 2019; Harley, 1998, 2016; Kelsey et al., 2007; Liu et al., 2023; Tong and Wilson, 2006). Meanwhile, the P–T path of the UHT granulite was suggested to evolve in a single Pan-African high-grade metamorphic event (Chen et al., 2023; Clark et al., 2019; Harley et al., 2009; Kelsey et al., 2007) or consist of two separate high-grade metamorphic events (Liu et al., 2023; Tong and Wilson, 2006; Wu et al., 2023). Thus, in order to clarify the timing of UHT metamorphism and P–T path of the UHT granulites associated with a single high-grade tectonothermal event or two separate metamorphic events, two typical UHT granulite samples in the region are selected for high-precision zircon SHRIMP U-Pb age dating to resolve this geological problem.

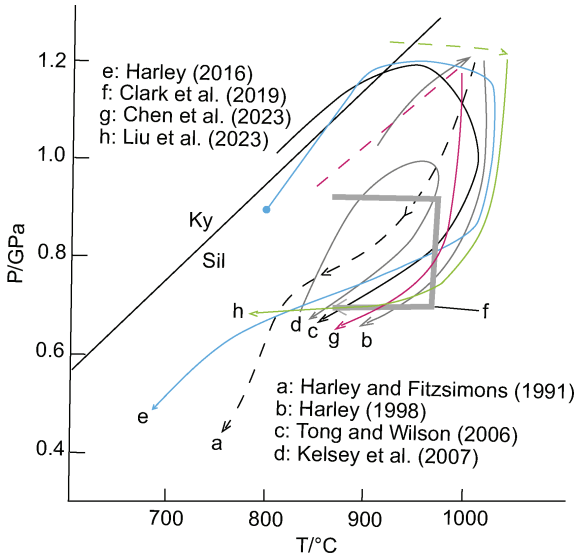

Figure 2 Various metamorphic P–T paths inferred by different researchers for the UHT granulites in the Rauer Group (modified after Tong et al., 2021). Ky indicates kyanite; Sil indicates sillimanite.

2 Geological setting

Located on the eastern margin of the early Palaeozoic Pan-African (550–500 Ma) high-grade mobile belt in Prydz Bay, the Rauer Group is about 10 km from the Archean (~2500 Ma) Vestfold Hills in the northeast and about 30 km from the Brattstrand Bluffs coast in the southwest (Harley, 1998). The Rauer Group belongs to a polymetamorphic high-grade terrain, and consists of Mesoproterozoic and Archean crustal domains (Figure 1a) (Harley and Kelly, 2007; Harley et al., 1998; Liu et al., 2021; Mikhalsky et al., 2019; Tong and Wilson, 2006). The Mesoproterozoic domain comprises intermediate to granitic orthogneisses with a Rb-Sr whole-rock isochron age of ~1100 Ma (Tingey, 1991) and zircon U-Pb ages of 1030–1000 Ma (Kinny et al., 1993), interleaving with the Filla Paragneiss associations (Filla superacrustal rocks) such as Fe-Al-rich metapelite, psammitic gneiss, garnet quartzite, leucogneiss, garnet-bearing calcsilicate and rare mafic granulite (Harley et al., 1995). The Filla superacrustal rocks have Mesoproterozoic Sm-Nd model ages of 1520–1160 Ma, and they were interpreted to represent a Mesoproterozoic sedimentary cover sequence which was deposited on the Archean orthogneiss basement (Sheraton et al., 1984). These rocks were considered to experience a medium-pressure granulite facies structural-metamorphic event in the late Proterozoic Grenvillian (~1000 Ma), with peak metamorphic conditions of 7–9 kbar and 820–860 ℃ and a clockwise P–T path of post-peak 2–4 kbar decompression (Harley, 1988; Harley and Fitzsimons, 1991). More recently, further geochronologcial data suggest that the Mesoproterozoic Filla Paragneiss unit underwent both the early Neoproterozoic Grenvillian (990–900 Ma) and the early Palaeozoic Pan-African

(550–500 Ma) metamorphic events (Kelsey et al., 2007; Liu et al., 2021), and thus belonged to part of the Rayner Complex (Alekseev et al., 2021; Liu et al., 2021; Mikhalsky et al., 2020).

The Archean domain consists of reworked Archean mafic-felsic orthogneisses hosting multiply deformed and metamorphosed Proterozoic mafic dykes (Dirks et al., 1994; Harley, 1987; Sims et al., 1994). The reworked Archean orthogneiss possesses magmatic crystallization ages of 3470 Ma, 3270 Ma and 2800 Ma (Harley et al., 1998; Kinny et al., 1993), and was considered to experience a phase of high-grade metamorphism prior to ~2500 Ma (Harley and Kelly, 2007). The Archean enderbitic orthogneiss hosts the Mather Paragneiss unit on Mather Peninsula (Figure 1b), and the unit consists of Mg-rich sapphirine-bearing metapelitic granulite, Mg-rich garnet-sillimanite-bearing paragneiss, orthopyroxene-sillimanite quartzite, garnet-bearing mafic granulite, forsteritic marble and calcsilicate granulite that experienced UHT metamorphism with peak P–T conditions of 10–12 kbar and 950–1050 ℃ and post-peak decompressional clockwise P–T path (Harley, 1998; Harley and Fitzsimons, 1991; Harley et al., 1995; Kelsey et al., 2007; Tong and Wilson, 2006). However, the timing of the UHT metamorphism and P–T path of the UHT granulites are still controversial, with distinct types of pre-peak and post-peak P–T evolution processes (Figure 2). For example, the UHT metamorphism was initially considered to likely occur in the Archean (Harley and Fitzsimons, 1991), and later it was thought to likely occur in the early Paleozoic Pan-African event (Harley, 1998; Hensen and Zhou, 1997; Kelsey et al., 2007). By contrast, some other researchers considered that the UHT metamorphism might have occurred in the early Neoproterozoic Grenvillian (~1000 Ma) event (Tong and Wilson, 2006; Wang et al., 2007). More recently, sapphirine-quartz-bearing UHT metapelitic granulites were reported from the Torckler Island (Harley et al., 2009). As some researchers considered that the Archean orthogneiss did not have a record of the Grenvillian (~1000 Ma) event (Harley et al., 1998; Hensen and Zhou, 1995, 1997), the UHT metamorphism was believed to occur in the late Neoproterozoic (~590 Ma) (Harley, 2014; Harley et al., 2009; Hokada et al., 2016) or in the early Paleozoic (530–510 Ma) (Chen et al., 2023; Clark et al., 2019; Liu et al., 2021). In addition, the P–T path of the UHT granulites was inferred to consist of two separate high-grade metamorphic events (Liu et al., 2023; Tong and Wilson, 2006; Wu et al., 2023) or to evolve in a single Pan-African high-grade metamorphic event (Chen et al., 2023; Clark et al., 2019; Harley, 1998; Harley et al., 2009; Kelsey et al., 2007).

The Rauer Group suffered multiple phases of structural deformation. The region was initially considered to experience at least four phases of high-grade structural deformation, in which the major deformation events (D1–D3) were suggested to occur prior to the intrusion of mafic dykes, whereas D4 deformation was thought to relate to granulite facied metamorphism of mafic dykes during the late Prorerozoic (~1000 Ma) (Harley, 1987; Kinny et al., 1993). Meanwhile, D4 deformation event was inferred to result in the formation of open to tight upright folding and the development of N-S-striking ductile shear zones in the region, while D5 deformation was associated with the intrusion of planar pegmatites (Harley, 1987). However, further structural deformation studies considered that most structures in the region were related to a phase of pervasive high-grade ductile shear deformation (D6) accompanied by granulite facies metamorphism at ~1000 Ma, and the pervasive development of planar high-strain zones, while early structures are locally preserved as refolded mafic granulite and felsic gneiss layers in lower-strain domains (Dirks et al., 1994; Sims et al., 1994). Throughout the Rauer Group, the regionally consistent steep southeast-plunging mineral elongation lineations are generally parallel to both fold axes and boudin necks (Figure 1d; Dirks and Wilson, 1995). Widespread D6 high-grade ductile shear deformation was then considered to occur in the early Paleozoic Pan-African (550–500 Ma) event (Dirks and Wilson, 1995; Sims and Wilson, 1997).

3 Samples and petrography

The Mather Paragneiss mainly occurs as folded metapelitic granulite layers and as interleaved rafts or discrete layers within the host enderbitic orthogneiss in a planar high-strain zone on Mather Peninsula (Figure 1b) (Harley, 1998). As both sapphirine-bearing metapelitic granulite and garnet-bearing mafic granulite experienced UHT metamorphism (Harley, 1998; Tong and Wilson, 2006), these two typical UHT granulites (samples LT59 and LT62) were selected for high-precision zircon SHRIMP U-Pb age dating (Figure 1b). The petrographic features for the two UHT granulite samples are described next.

Sample LT59 is a coarse-grained sapphirine-bearing metapelitic granulite with apparent foliated structures (Figure 3a). The sample is composed mainly of garnet, orthopyroxene, sillimanite, sapphirine, cordierite, biotite, plagioclase, K-feldspar, perthite, and minor spinel, and accessary minerals such as zircon and monazite. As the rock does not contain quartz, it is Si-unsaturated. Coarse garnet porphyroblast contains some small oriented inclusion assemblage of sillimanite-sapphirine-plagioclase-biotite close to the garnet rim, with the development of post-peak decompression reaction corona assemblage of spinel-cordierite-sillimanite (Figure 3c). In places, sapphirine grain and sapphirine-orthopyroxene overgrowth occurs in the matrix, and post-peak fine-grained symplectite assemblage of orthopyroxene-cordierite occurs on garnet grain, besides the garnet contains some oriented biotite-sillimanite-plagioclase inclusions (Figure 3c). The mineral assemblages and reaction textures suggest that the UHT metapelitic granulite experienced post-peak at least two-stage decompression and multi-stage metamorphic evolution processes (Harley, 1998; Harley and Fitzsimons, 1991; Tong and Wilson, 2006).

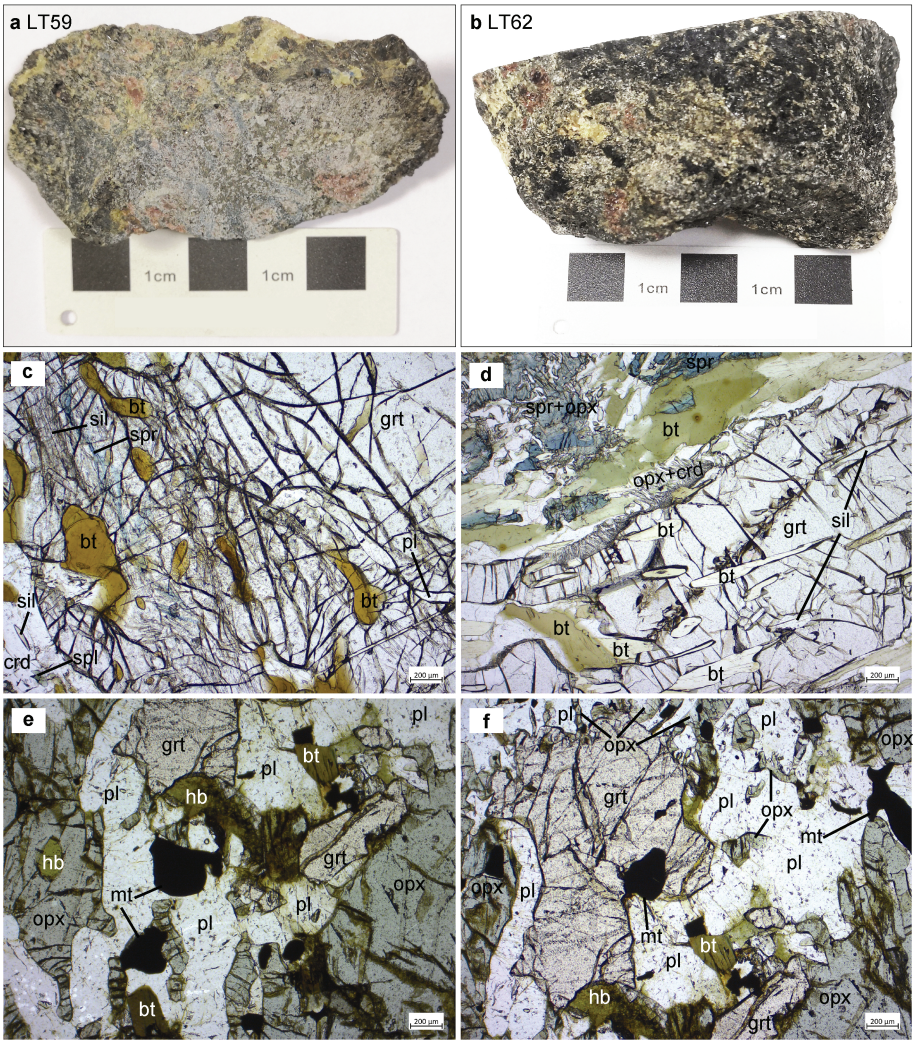

Figure 3 Hand sample photographs and microphotographs of the UHT granulites in the Rauer Group. **a**, spr-bearing UHT metapelitic granulite (sample LT59); **b**, grt-bearing UHT mafic granulite with "white-eye socket" decompression texture (sample LT62); **c**, garnet porphyroblast contains aligned spr-sil-bt inclusions and spl-crd-sil reaction rim (sample LT59); **d**, garnet porphyroblast contains aligned sil-bt-pl inclusions and opx-crd reaction rim and opx-spr intergrowth in the matrix (sample LT59); **e**, orthopyroxene grain contains small hornblende inclusion and garnet overgrowth (sample LT62); **f**, garnet porphyroblast develops opx-pl-mt reaction rim texture (sample LT62). Mineral abbreviations: grt, garnet; opx, orthopyroxene; sil, sillimanite; spr, sapphirine; spl, spinel; crd, cordierite; bt, biotite; pl, plagioclase; hb, hornblende; mt, magnetite.

Sample LT62 is a garnet-bearing mafic granulite with the development of typical "white-eye socket" decompression textures on garnet grain (Figure 3b), and consists mainly of garnet, orthopyroxene, hornblende, plagioclase, and minor biotite, clinopyroxene, quartz, K-feldspar and opaque mineral magnetite. The orthopyroxene grain contains small pre-peak hornblende inclusion assemblage, and the microtexture indicates peak mineral assemblage of garnet-orthopyroxene-plagioclase-clinopyroxene with post-peak small garnet overgrowth around orthopyroxene grain (Figure 3e). The garnet porphyroblast develops post-peak "white-eye-socket" corona assemblage of orthopyroxene-plagioclase-magnetite, and later mineral assemblage of hornblende-plagioclase (Figure 3f), indicating post-peak important retrograde decompression processes from granulite to amphibolite facies, likely accompanied by a minor cooling. The previous studies support that the garnet-bearing mafic granulites experienced UHT metamorphism together with the sapphirine-bearing metapelitic granulites in the region (Chen et al., 2023; Tong and Wilson, 2006).

4 Zircon SHRIMP U-Pb ages

Zircon grains were separated using conventional magnetic and heavy liquid techniques for the two UHT granulites, and followed by hand-picking under a binocular microscope. The zircon grains were then mounted in an epoxy resin disc along with the TEMORA zircon standard and polished to expose grain centres. The zircon morphology

and internal structure were documented with transmitted and reflected light microphotographs and cathodoluminenscene (CL) images. The U-Th-Pb isotope analyses of zircon grains were undertaken using the SHRIMP II ion microprobe machine at the Beijing SHRIMP Centre, Chinese Academy of Geological Sciences, using the standard operating conditions outlined by Williams (1998). Th-U-Pb ratios were determined relative to the TEMORA standard zircon. Pb_c and Pb^* represent the common and radiogenic portions, respectively, and common Pb was corrected using measured ^{204}Pb. Software SQUID 1.03 and ISOPLOT 3.23 (Ludwig, 2001, 2003) were used for data processing. The age uncertainties for individual analyses are reported as one standard deviation (1σ), and the calculated weighted mean $^{206}Pb/^{238}U$ ages are quoted at the 95% confidence level. Representative CL images of zircons in the two UHT granulite samples LT59 and LT62 are shown in Figure 4, and zircon SHRIMP analysis data and age results are shown in Table 1, Table 2, Figure 5 and Figure 6, respectively.

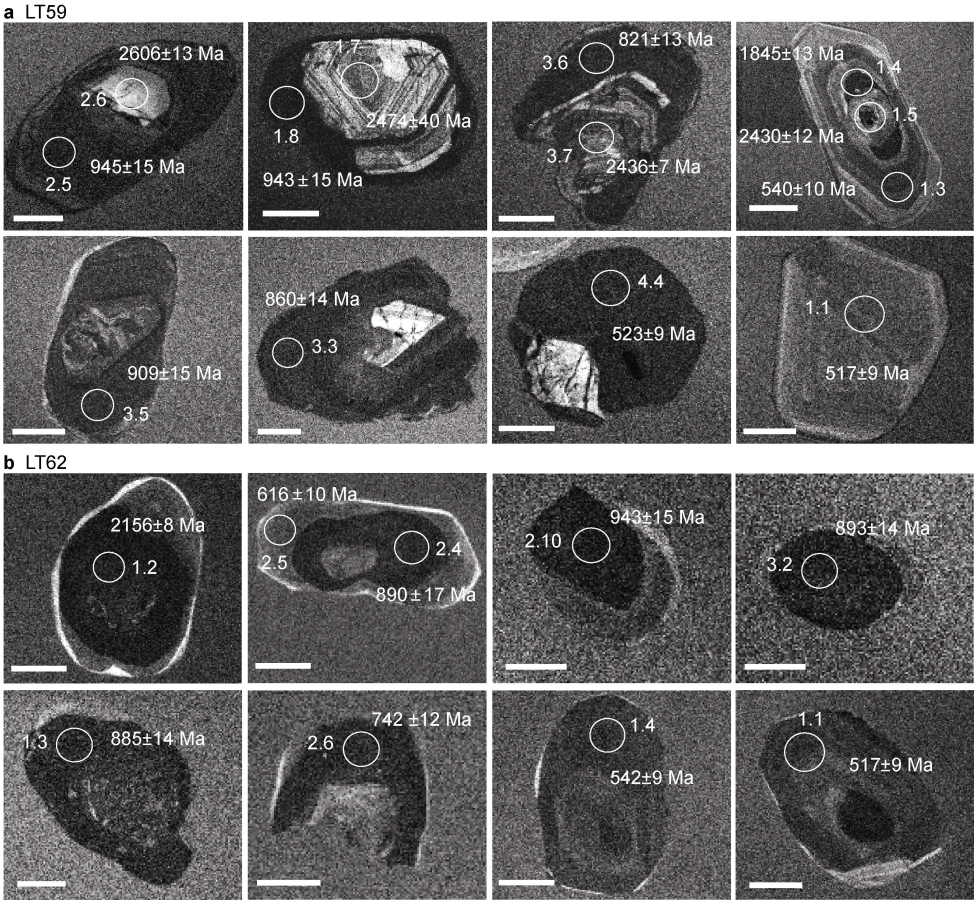

Figure 4 The CL images for representative zircons in the UHT granulites (**a**, sample LT59; **b**, sample LT62) in the Rauer Group.

Table 1 SHRIMP U-Pb analyses of zircons from sapphirine-bearing UHT metapelitic granulite (sample LT59)

Spot	$^{206}Pb_c$/%	U	Th	Th/U	$^{207}Pb^*/^{206}Pb^*$	%	$^{207}Pb^*/^{235}U$	%	$^{206}Pb^*/^{238}U$	%	$^{207}Pb/^{206}Pb$/Ma	1s err	$^{208}Pb/^{232}Th$/Ma	1s err	$^{206}Pb/^{238}U$/Ma	1s err
LT59-1.1	0.33	297	111	0.39	0.0557	2.8	0.64	3.3	0.0835	1.8	440.3	61.4	502.9	17.6	516.7	8.9
LT59-1.2	0.43	293	107	0.38	0.0551	3.3	0.64	3.8	0.0840	1.8	414.5	73.5	469.2	21.0	519.9	9.0
LT59-1.3	0.07	573	163	0.29	0.0572	1.6	0.69	2.5	0.0873	1.9	497.7	36.0	510.3	15.1	539.8	9.9
LT59-1.4	0.13	1005	91	0.09	0.1128	1.0	3.62	2.0	0.2330	1.8	1845.3	17.7	1685.2	65.3	1350.3	21.6
LT59-1.5	0.27	564	223	0.41	0.1576	0.7	6.54	1.9	0.3008	1.7	2430.0	12.4	2167.0	53.6	1695.2	25.9
LT59-1.6	0.00	705	35	0.05	0.1573	0.4	8.77	1.8	0.4045	1.7	2426.8	6.2	2132.5	48.8	2189.7	31.8
LT59-1.7	0.10	308	73	0.24	0.1617	0.6	10.15	1.9	0.4555	1.8	2473.5	10.2	2216.3	62.3	2419.4	35.4
LT59-1.8	0.10	1386	65	0.05	0.0668	0.7	1.45	1.8	0.1575	1.7	830.6	14.1	952.4	56.1	942.9	15.0
LT59-2.1	−0.06	360	135	0.39	0.0578	1.7	0.69	2.4	0.0866	1.8	521.6	36.3	525.8	12.9	535.3	9.1
LT59-2.2	0.38	264	39	0.15	0.0546	3.5	0.63	4.0	0.0831	1.8	396.0	78.7	346.1	45.4	514.6	9.0

Continued

Spot	$^{206}Pb_c$/%	U	Th	Th/U	$^{207}Pb^*/^{206}Pb^*$	%	$^{207}Pb^*/^{235}U$	%	$^{206}Pb^*/^{238}U$	%	$^{207}Pb/^{206}Pb$/ Ma	1s err	$^{208}Pb/^{232}Th$/ Ma	1s err	$^{206}Pb/^{238}U$/ Ma	1s err
LT59-2.3	0.08	762	467	0.63	0.1461	0.5	5.84	1.8	0.2897	1.7	2300.7	7.7	1323.6	59.1	1640.1	24.8
LT59-2.4	0.20	384	146	0.39	0.0560	2.6	0.57	3.2	0.0741	1.8	451.8	58.8	421.1	14.8	461.0	8.0
LT59-2.5	0.05	1010	106	0.11	0.0689	0.7	1.50	1.9	0.1578	1.7	895.5	14.7	898.3	23.3	944.7	15.1
LT59-2.6	0.09	185	51	0.28	0.1750	0.8	9.44	2.0	0.3909	1.8	2606.5	12.8	2108.0	50.8	2127.1	33.1
LT59-3.1	0.06	865	79	0.09	0.0690	0.8	1.41	1.9	0.1487	1.7	898.5	16.3	821.7	24.4	893.6	14.3
LT59-3.2	0.24	291	76	0.27	0.0564	2.3	0.66	2.9	0.0851	1.8	468.2	51.8	475.5	16.5	526.6	9.1
LT59-3.3	0.00	1365	134	0.10	0.0677	0.6	1.33	1.8	0.1427	1.7	859.3	13.0	830.3	17.8	859.9	13.7
LT59-3.4	0.05	953	81	0.09	0.0692	0.8	1.43	1.9	0.1502	1.7	906.0	16.7	846.5	21.8	902.1	14.4
LT59-3.5	0.00	1109	100	0.09	0.0691	0.9	1.44	1.9	0.1514	1.7	902.7	18.6	862.1	26.6	908.7	14.5
LT59-3.6	0.06	1255	92	0.08	0.0657	0.8	1.23	1.9	0.1357	1.7	796.9	16.3	746.7	35.2	820.5	13.1
LT59-3.7	−0.01	497	320	0.66	0.1582	0.4	8.86	1.8	0.4064	1.7	2436.2	6.9	2312.0	41.6	2198.4	32.1
LT59-4.1	0.02	1987	475	0.25	0.1476	0.2	7.07	1.7	0.3472	1.7	2318.2	4.2	1942.6	36.0	1921.2	28.1
LT59-4.2	−0.06	829	90	0.11	0.0583	1.3	0.62	2.1	0.0771	1.7	542.3	27.6	470.8	13.8	478.8	8.0
LT59-4.3	0.02	415	129	0.32	0.0568	2.1	0.68	2.7	0.0874	1.8	483.2	45.8	518.4	13.7	540.1	9.1
LT59-4.4	0.07	949	55	0.06	0.0565	1.1	0.66	2.1	0.0846	1.7	472.0	25.1	481.8	27.3	523.3	8.6
LT59-4.5	0.13	773	232	0.31	0.0554	2.0	0.64	2.7	0.0836	1.7	430.0	45.7	461.7	10.4	517.6	8.6
LT59-4.6	−0.38	387	149	0.40	0.0616	3.2	0.69	3.7	0.0809	1.8	659.1	69.6	504.3	22.2	501.5	8.7

Table 2 SHRIMP U-Pb analyses of zircons from garnet-bearing UHT mafic granulite (sample LT62)

Spot	$^{206}Pb_c$/%	U	Th	Th/U	$^{207}Pb^*/^{206}Pb^*$	%	$^{207}Pb^*/^{235}U$	%	$^{206}Pb^*/^{238}U$	%	$^{207}Pb/^{206}Pb$/ Ma	1s err	$^{208}Pb/^{232}Th$/ Ma	1s err	$^{206}Pb/^{238}U$/ Ma	1s err
LT62-1.1	0.14	593	68	0.12	0.0575	1.8	0.66	2.5	0.0835	1.7	509.4	38.6	474.8	26.4	516.8	8.7
LT62-1.2	0.03	1372	215	0.16	0.1344	0.5	4.48	1.8	0.2421	1.7	2155.9	8.2	2298.2	42.7	1397.4	21.7
LT62-1.3	0.01	3339	73	0.02	0.0675	0.4	1.37	1.7	0.1472	1.7	854.0	8.3	863.7	36.4	885.3	14.0
LT62-1.4	0.01	863	90	0.11	0.0569	1.2	0.69	2.1	0.0877	1.7	489.0	26.4	531.0	18.8	541.9	8.9
LT62-1.5	0.05	2446	112	0.05	0.0668	0.5	1.13	1.8	0.1222	1.7	831.5	11.0	973.1	27.0	743.5	11.9
LT62-1.6	0.04	2548	97	0.04	0.0661	0.5	1.28	1.8	0.1400	1.7	811.0	10.8	752.6	30.2	844.7	13.4
LT62-1.7	0.04	1081	334	0.32	0.1452	0.4	6.58	1.7	0.3287	1.7	2290.6	6.2	2167.8	39.8	1832.2	27.1
LT62-1.8	−0.05	754	88	0.12	0.0582	1.2	0.70	2.1	0.0873	1.7	536.3	26.2	547.6	18.3	539.3	8.9
LT62-1.9	0.02	1715	312	0.19	0.1201	0.3	3.70	1.7	0.2235	1.7	1958.1	6.1	2109.1	37.8	1300.2	20.0
LT62-2.1	0.00	579	58	0.10	0.0582	1.2	0.69	2.1	0.0855	1.7	538.0	26.8	519.8	15.0	528.6	8.8
LT62-2.2	−0.02	2223	160	0.07	0.0735	0.5	1.33	1.8	0.1314	1.7	1027.9	9.6	1448.8	43.7	796.1	13.0
LT62-2.3	0.01	590	50	0.09	0.0573	1.6	0.65	2.4	0.0828	1.7	502.1	35.2	503.7	18.2	513.1	8.6
LT62-2.4	0.05	1784	48	0.03	0.0660	1.1	1.35	2.3	0.1481	2.0	804.9	22.3	734.1	44.4	890.2	16.5
LT62-2.5	−0.03	604	49	0.08	0.0595	1.1	0.82	2.1	0.1002	1.8	585.4	23.9	634.8	28.0	615.9	10.4
LT62-2.6	0.05	1512	73	0.05	0.0669	0.7	1.13	1.8	0.1220	1.7	835.8	13.7	637.4	29.6	742.3	11.9
LT62-2.7	0.09	649	59	0.09	0.0568	1.3	0.69	2.1	0.0881	1.7	482.4	28.1	494.2	22.7	544.2	9.0
LT62-2.8	0.10	1394	52	0.04	0.0663	0.7	1.21	1.9	0.1320	1.8	816.9	15.0	606.4	46.4	799.3	13.3
LT62-2.9	0.26	591	67	0.12	0.0566	1.6	0.70	2.3	0.0895	1.7	474.8	34.8	454.3	27.6	552.7	9.1
LT62-2.10	0.00	2043	58	0.03	0.0689	0.5	1.50	1.8	0.1575	1.7	894.7	10.2	915.0	26.3	943.1	14.8
LT62-3.1	0.00	2910	89	0.03	0.0680	0.4	1.35	1.7	0.1442	1.7	868.4	8.1	853.8	18.9	868.4	13.7
LT62-3.2	0.03	1756	75	0.04	0.0693	0.6	1.42	1.8	0.1485	1.7	907.8	12.0	854.5	24.4	892.6	14.2
LT62-3.3	0.00	911	51	0.06	0.0582	1.1	0.70	2.0	0.0869	1.7	538.0	23.8	542.4	21.0	537.5	8.8
LT62-3.4	0.04	3467	113	0.03	0.0677	0.6	1.39	1.8	0.1491	1.7	859.4	12.9	807.8	28.7	896.1	14.1
LT62-3.5	0.10	673	65	0.10	0.0587	1.5	0.67	2.3	0.0831	1.7	556.1	32.4	475.7	26.8	514.9	8.5
LT62-3.6	0.04	2338	38	0.02	0.0611	0.5	0.92	1.8	0.1087	1.7	643.2	11.8	587.8	44.7	665.4	10.7
LT62-3.7	0.00	1866	65	0.04	0.0666	0.6	1.19	1.8	0.1292	1.7	824.4	12.5	722.7	27.8	783.1	12.6

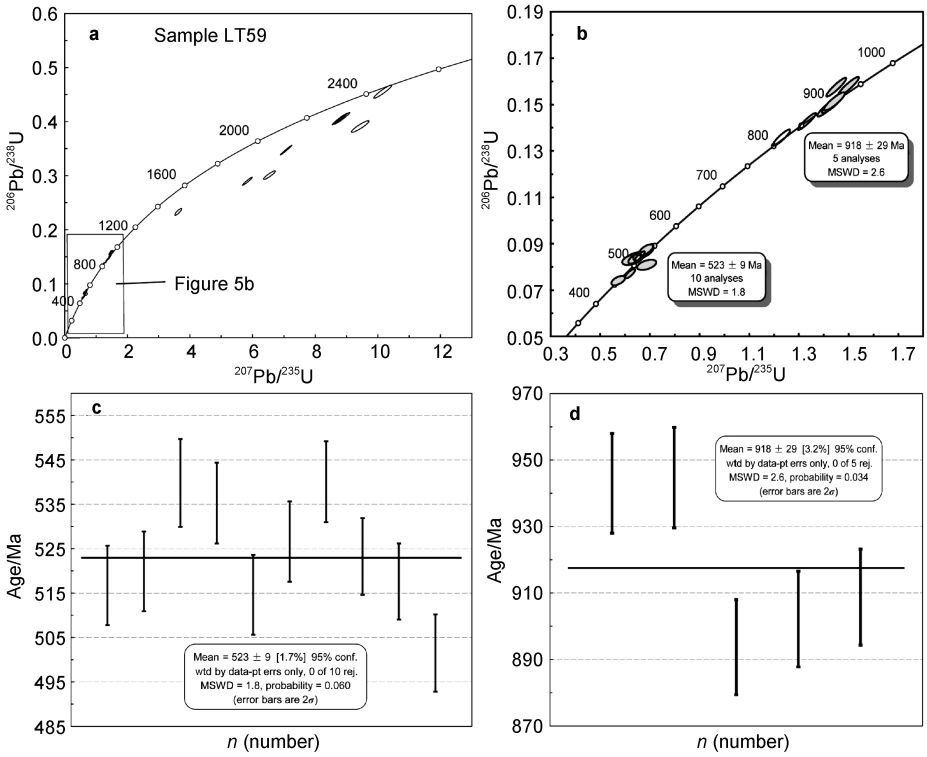

Figure 5 **a**, SHRIMP U-Pb concordia diagram of zircons in the sapphirine-bearing UHT metapelitic granulite (sample LT59); **b**, U-Pb concordia age plot of Grenvillian and Pan-African metamorphic zircon mantles; **c**, weighted U-Pb mean age of Pan-African metamorphic zircon rims; **d**, weighted U-Pb mean age of Grenvillian metamorphic zircon mantles. Abbreviations: conf, confidence; wtd, weighted; rej, rejection.

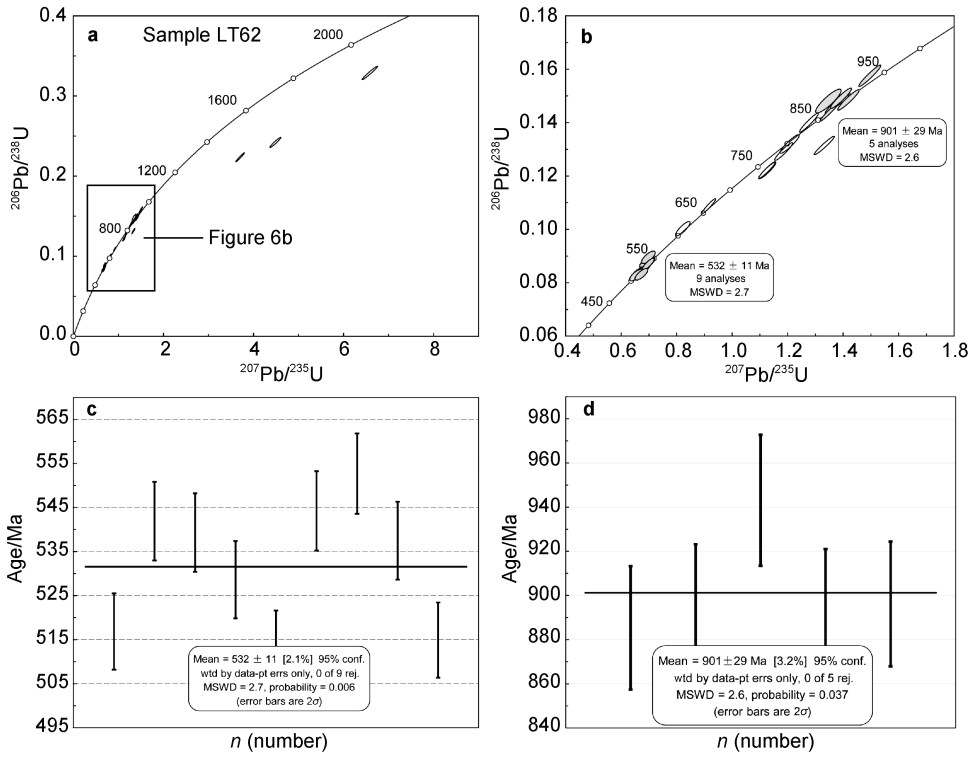

Figure 6 **a**, SHRIMP U-Pb concordia diagram of zircons in the garnet-bearing UHT mafic granulite (sample LT62); **b**, U-Pb concordia age plot of Grenvillian and Pan-African metamorphic zircon mantles; **c**, weighted U-Pb mean age of Pan-African metamorphic zircon rims; **d,** weighted U-Pb mean age of Grenvillian metamorphic zircon mantles. Abbreviations: conf, confidence; wtd, weighted; rej, rejection.

Zircons in the sapphirine-bearing UHT metapelitic granulite (sample LT59) mostly are oval to spherical or prismatic in shape and 80–260 μm in length, with length to width ratios of 1∶1 to 3∶1. Their CL images show that the zircon grains have core-mantle or core-mantle-rim internal structures or new homogenous growth structure (Figure 4). The zircon cores are commonly light colour with magmatic oscillatory or rhythmic zoning, while the mantles are often dark or grey colour with planar zoning features. The rims or newly grown zircons are light grey colour with apparent growth zoning (Figure 4). A total of 27 analyses were undertaken on 17 zircon grains, with U concentrations of 185–1987 ppm and Th/U ratios of 0.05–0.66 (Table 1). The zircon cores mostly have relatively high Th/U ratios of 0.24–0.66, belonging to detrital magmatic zircons with $^{207}Pb/^{206}Pb$ ages of 2300.7–2606.5 Ma, except that one detrital zircon core has a low Th/U ratio of 0.05 and a $^{207}Pb/^{206}Pb$ age of 2426.8 Ma (Table 1). The dark zircon mantles all have low Th/U ratios of 0.05–0.11, belonging to metamorphic overgrowth zircons with $^{206}Pb/^{238}U$ ages of 820.5–944.7 Ma, except that one zircon mantle has a $^{207}Pb/^{206}Pb$ age of 1845.3 Ma (Table 1), which is inferred to likely represent a mixing age. Given that two ages of 820.5 Ma and 859.9 Ma could have been affected or reset by the Pan-African thermal event, the other five zircon mantles yielded a weighted $^{206}Pb/^{238}U$ mean age of 918±29 Ma (Figure 5). The zircon rims and newly grown grains have Th/U ratios of 0.06–0.40, belonging to both metamorphic and magmatic zircons with $^{206}Pb/^{238}U$ ages of 461.0–540.1 Ma (mainly between 502–540 Ma) (Table 1). As two ages of 461.0 and 478.8 Ma apparently deviated from the 502–540 Ma, the other ten analyses produced a weighted $^{206}Pb/^{238}U$ mean age of 523±9 Ma (Figure 5).

Zircons in the garnet-bearing UHT mafic granulite (sample LT62) mostly are oval to spherical or short prismatic in shape and 40–150 μm in grain size, with length to width ratios of 1∶1 to 2∶1. In the CL images, the zircon grains exhibit core-mantle-rim or core-mantle internal structures (Figure 4). The zircon cores are usually grey to light grey colour with detrital genesis, while the mantles or newly grown cores are often dark colour likely associated with first recrystallization. The rims usually show grey colour with narrow to wide zoning (Figure 4). A total of 26 analyses were undertaken on 25 zircon grains, with U concentrations of 579–3467 ppm and Th/U ratios of 0.02–0.32 (Table 2). The analyses of three representative zircon cores show that they have relatively high Th/U ratios of 0.16–0.32, belonging to typical magmatic zircons with $^{207}Pb/^{206}Pb$ ages of 1958.1–2290.6 Ma. The dark zircon mantles have very low Th/U ratios of 0.02–0.07, belonging to typical metamorphic zircons with $^{206}Pb/^{238}U$ ages of 665.4–943.1 Ma (Table 2). Given that the ages of 665.4–868.4 Ma might have been affected or reset by the Pan-African thermal event, the other five zircon mantles produced a weighted $^{206}Pb/^{238}U$ mean age of 901±29 Ma (Figure 6). The zircon rims have relatively low Th/U ratios of 0.06–0.12, belonging to metamorphic zircons with $^{206}Pb/^{238}U$ ages of 513.1–615.9 Ma (mostly between 513–553 Ma) (Table 2). As the age of 615.9 Ma remarkably deviated from the ages of 513–553 Ma, the other 9 analyses yielded a weighted $^{206}Pb/^{238}U$ mean age of 532±11 Ma (Figure 6).

5 Discussion and conclusions

5.1 Interpretation of zircon SHRIMP U-Pb ages

The UHT granulites in the Rauer Group experienced a multi-stage evolution history, including sapphirine-orthopyroxene-sillimanite-garnet-bearing Mg-Al-rich metapelitic granulite, garnet-sillimanite/kyanite-bearing Fe-Al-rich metapelitic granulite and garnet-clinopyroxene-orthopyroxene-bearing mafic granulite (Harley, 1998; Harley and Fitzsimons, 1991; Kelsey et al., 2007; Tong and Wilson, 2006). However, till recently, a long-standing debate exists regarding the timing of UHT metamorphism (Harley, 1998; Harley et al., 2009; Hokada et al., 2016; Kelsey et al., 2007; Tong and Wilson, 2006; Wang et al., 2007) and the P–T path of the UHT granulites involves a single Pan-African metamorphic event (Chen et al., 2023; Clark et al., 2019; Harley et al., 2009; Kelsey et al., 2007) or two separate high-grade metamorphic events (Liu et al., 2023; Tong and Wilson, 2006; Wu et al., 2023). For instance, the UHT metamorphism was considered to occur in the early Neoproterozoic (~1000 Ma) (Tong and Wilson, 2006; Wang et al., 2007; Wu et al., 2023), or in the late Neoproterozoic (~590 Ma) (Harley, 2014; Harley et al., 2009; Hokada et al., 2016), or in the early Paleozoic (540–510 Ma) (Clark et al., 2019; Kelsey et al., 2007; Liu et al., 2021; Sim and Wilson, 1997). In addition, the protolith sedimentation of the UHT metapelitic granulites was inferred to occur in the Neoproterozoic (Hokada et al., 2016; Kelsey et al., 2008; Liu et al., 2021).

In the multi-phase metamorphic regions, zircons usually have multi-stage core-mantle-rim internal structures, and thus they record the multi-phase evolution history of their host rocks (Wu and Zheng, 2004). Zircons in the two UHT granulites in this study also show typical core-mantle-rim internal structures (Figure 4). For the UHT metapelitic granulite sample LT59, a weighted $^{206}Pb/^{238}U$ mean age of 918±29 Ma produced from the five metamorphic zircon mantles indicates that the UHT metapelitic granulite experienced a phase of high-grade metamorphism during the early Neoproterozoic (Figure 5). Whereas a weighted $^{206}Pb/^{238}U$ mean age of 523±9 Ma yielded from the ten zircon rims and newly grown zircons suggests that an overprinting high-grade metamorphism accompanied by partial melting occurred in the early Paleozoic (Figure 5). In addition, the detrital zircon cores with $^{207}Pb/^{206}Pb$ ages of 2301–2607 Ma (mainly between 2430–2470 Ma) show that their source protoliths were derived from the eroded late Archean to early Paleoproterozoic igneous and metamorphic rocks. Likewise, for the UHT mafic granulite sample LT62, a weighted $^{206}Pb/^{238}U$ mean age of 901±29 Ma produced

from the five metamorphic zircon mantles indicates that the UHT mafic granulite suffered an episode of high-grade metamorphism in the early Neoproterozoic (Figure 6). Again, a weighted $^{206}Pb/^{238}U$ mean age of 532±11 Ma yielded from the nine zircon rims shows that an overprinting high-grade metamorphism occurred in the early Paleozoic (Figure 6). Additionally, the inherited zircon cores with the $^{207}Pb/^{206}Pb$ ages of 1958–2291 Ma suggest that its source protolith was likely formed in the late Paleoproterozoic.

The above new zircon SHRIMP U-Pb age data obtained from the two typical UHT granulites in the Rauer Group support that the UHT granulites underwent both the early Neoproterozoic (920–900 Ma) and the early Paleozoic (530–510 Ma) metamorphic events, thus the P–T path of the UHT granulites actually should consist of two separate high-grade metamorphic events rather than a single Pan-African high-grade event. Therefore, this is consistent with the inference of Liu et al (2023). A weighted zircon SHRIMP $^{207}Pb/^{206}Pb$ mean age of 995±15 Ma yielded from metamorphic zircon mantles in a sapphirine-bearing UHT metapelitic granulite in the region also support that the UHT granulite suffered a phase of high-grade metamorphism in the early Neoproterozoic (1000–900 Ma) (Wang et al., 2007). Since the inclusion assemblages in garnet and orthopyroxene porphyroblasts in the UHT granulites in the region represent an early prograde metamorphic stage, and correspond to the prograde stage of the P–T path of the UHT granulites, we infer that the early Neoproterozoic high-grade event should be related to the prograde metamorphic stage prior to peak UHT metamorphism, different from the interpretation of Tong and Wilson (2006) and Wu et al (2023).

Furthermore, as sapphirine-orthopyroxene and sapphirine-orthopyroxene-sillimanite symplectite assemblages occur on peak garnet grains in the UHT metapelitic granulites (Harley, 1998; Tong et al., 2021), and indicate that peak UHT metamorphism should occur during the first decompression after pressure peak, consistent with that of Tong and Wilson (2006). Thus, here we think that peak UHT metamorphism belongs to an overprinting Pan-African high-grade metamorphic event. Although some workers considered that the UHT metamorphism occurred in the late Neoproterozoic (590–570 Ma) (Harley, 2014; Harley et al., 2009; Hokada et al., 2016; Liu et al., 2023) or in the early Paleozoic (540–520 Ma) (Chen et al., 2023; Clark et al., 2019; Kelsey et al., 2007; Liu et al., 2021), zircon U-Pb and monazite U-Th-Pb ages from the UHT metapelitic granulites in the region show that the Pan-African high-grade metamorphic event occurred in an age range of 580–460 Ma (Hokada et al., 2016; Kelsey et al., 2007; Liu et al., 2023). Therefore, we prefer that the overprinting Pan-African UHT metamorphic event should be a protracted orogenic event spanning from the late Neoproterozoic to the early Paleozoic (580–460 Ma).

In addition, some debates also exist regarding the deposition age of the UHT metapelitic granulites in the region. For instance, according to the zircon SHRIMP U-Pb age data, the protolith sedimentation of the paragneisses in the Rauer Group was initially considered to occur before the intrusion age of ~1000 Ma orthogneiss (Kinny et al., 1993). However, later some researchers inferred that the protolith of UHT metapelitic granulites in the region was deposited in the late Neoproterozoic (Hokada et al., 2016; Kelsey et al., 2008; Liu et al., 2021). Based on the above new zircon U-Pb age data, because the UHT metapelitic granulite also experienced the early Neoproterozoic (1000–900 Ma) high-grade metamorphic event like the Filla Paragneiss, it is logically inferred that the protolith sedimentation of the UHT Mather paragneiss should occur in the Mesoproterozoic before the ~1000 Ma. This suggestion is consistent with the inference of Dirks and Wilson (1995) who considered that the UHT metapelites might be part of the Mesoproterozoic sedimentary pile and possibly represent a restricted Mg-rich facies at the base of the sequence. Although there is no ~1000 Ma age record in the Archean domain orthogneiss in the Rauer Group (Harley et al., 1998; Hensen and Zhou, 1995, 1997; Hokada et al., 2016; Liu et al., 2021), the new zircon U-Pb age data support that the UHT metapelitic granulites also suffered the early Neoproterozoic (1000–900 Ma) high-grade metamorphic event. The early prograde stage in the UHT metapelitic granulites involves kyanite to sillimanite transformation (Harley et al., 2009; Tong and Wilson, 2006), which is consistent with the prograde stage in the Filla Paragneiss (kyanite to sillimanite transformation occurred in the early Neoproterozic) (Harley, 2014). This indirectly supports that the protolith sedimentation of the Mather paragneiss should occur at least before the ~1000 Ma.

5.2 Tectonic implications for polymetamorphism of the UHT granulites

The Rauer Group is located on the eastern margin of the early Paleozoic (~530 Ma) Pan-African high-grade tectonic mobile belt (Prydz Belt) in East Antarctica, and consists of the Mesoproterozoic crustal domain and Archean crustal domain (Harley and Kelly, 2007; Harley et al., 1998; Liu et al., 2021; Tong and Wilson, 2006). The Rauer Group was considered to represent a polymetamorphic terrain (Rauer Terrain), and experienced an early Neoproterozoic Grenvillian (1000–900 Ma) high-grade tectonic event (Rauer Tectonic Event) and an early Paleozoic Pan-African (~530 Ma) tectonic event (Prydz Tectonic Event) (Harley and Kelly, 2007). The Mesoproterozoic supracrustal rocks (Filla Paragneiss) have been suggested to suffer both the early Neoproterozoic Grenvillian and the early Palaeozoic Pan-African metamorphic events (Kelsey et al., 2007; Liu et al., 2021). However, up to the present, a debate still exists regarding the timing of UHT metamorphism and tectonic settings and whether or not the UHT Mather Paragneiss in the Archean crustal domain experienced the early Neoproterozoic Grenvillian metamorphism (Harley, 1998, 2014; Hensen

and Zhou, 1997; Hokada et al., 2016; Kelsey et al., 2007; Liu et al., 2021; Tong and Wilson, 2006; Wilson et al., 2007). For example, the UHT metamorphism was inferred to occur in the early Neoproterozoic (Tong and Wilson, 2006; Wang et al., 2007; Wu et al., 2023), or in the early Paleozoic (Chen et al., 2023; Clark et al., 2019; Kelsey et al., 2007; Liu et al., 2021; Sim and Wilson, 1997), or in the late Neoproterozoic (Harley, 2014; Harley et al., 2009; Hokada et al., 2016; Liu et al., 2023). In addition, the P–T history of the UHT granulites was considered to consist of two separate high-grade metamorphic events (Liu et al., 2023; Tong and Wilson, 2006; Wu et al., 2023) or just evolve in a single high-grade tectonic event (Chen et al., 2023; Clark et al., 2019; Harley, 2014; Harley et al., 2009; Kelsey et al., 2007). Therefore, this resulted in different inferences for the tectonic nature of the region and the Prydz Belt, for instances, some workers considered that the UHT metamorphism was formed in a single Pan-African metamorphic event associated with the final assembly of Gondwana supercontinent (Harley, 2014; Hensen and Zhou, 1997; Hokada et al., 2016; Kelsey et al., 2008; Liu et al., 2021; Wang et al., 2022), whereas others thought that the Pan-African metamorphic event reflected the development of ductile shear zones and a widespread intraplate reworking (Liu et al., 2023; Tong et al., 2014, 2019; Wang et al, 2008; Wilson et al., 2007).

The new zircon SHRIMP U-Pb age data obtained from the two UHT granulites in the Mather Paragneiss further support that the UHT Mather Paragneiss experienced polymetamorphism, namely, the UHT granulites suffered both the early Neoproterozoic Grenvillian (1000–900 Ma) and the late Neoproterozoic to the early Paleozoic Pan-African (580–460 Ma) high-grade metamorphic events like the Filla Paragneiss. Thus, both the Mather Paragneiss and the Filla Paragneiss might have shared P–T paths (Tong and Wilson, 2006), which consist of two separate high-grade metamorphic events. As suggested above, the early Neoproterozoic metamorphic event may be associated with the prograde metamorphic stage of the P–T path of the UHT granulites, whereas the late Neoproterozoic to the early Paleozoic Pan-African metamorphic event may be responsible for the UHT metamorphism and post-peak retrograde metamorphism, indicating that the Pan-African event belongs to be an overprinting and protracted tectonic event. Recently, the mafic dykes in the adjacent Vestfold Hills were reported to suffer an early Neoproterozoic Grenvillian (960–940 Ma) granulite facies high-grade metamorphic event (Liu et al., 2014), suggesting that the Rauer Terrain might have formed by juxtaposition with the Archean Vestfold block during the early Neoproterozoic (Alekseev et al., 2021; Harley et al., 1995, 1998; Kinny et al., 1993). Although some workers noticed that there was no record of ~1000 Ma ages in the orthogneiss from the Archean crustal domain (Harley et al., 1998; Hensen and Zhou, 1995, 1997; Hokada et al., 2016; Kinny et al., 1993; Liu et al., 2021), preliminary zircon U-Pb metamorphic age data (1000–900 Ma) (authors' unpublished data) recently yielded from the country orthogneiss of the UHT granulites further support that the Archean orthogneiss also experienced the early Neoproterozoic Grenvillian high-grade metamorphism together with the UHT granulites in the region. Therefore, the early Neoproterozoic Grenvillian (1000–900 Ma) metamorphic event may be related to the assembly of Rodinia supercontinent, whilest the late Neoproterozoic to early Paleozoic Pan-African (580–460 Ma) metamorphic event may be a protracted overprinted orogenic event, and may actually reflect an important intracontinental reworking.

The new SHRIMP zircon U-Pb age evidence supports that the UHT granulites in the Rauer Group experienced polymetamorphism consisting of two separate high-grade metamorphic events such as the early Grenvillian (1000–900 Ma) and second Pan-African (580–460 Ma) events. Generally speaking, if the high-grade metamorphic rocks underwent two separate high-grade metamorphic events, their P–T path should consist of two P–T path loops rather than a single continuous P–T path loop, similar to that of the garnet-bearing mafic granulite from the Søstrene Island in the southwestern Prydz Bay (Hensen et al., 1995), just about 15 km west of the Larsemann Hills. Therefore, the present P–T paths of the UHT granulites in the Rauer Group consisting mostly of a single successive path loop (Figure 2) need substantially to be re-examined and further clarified.

Acknowledgements The field work was carried out with logistic support from the 27th and 33rd Chinese National Antarctic Research Expedition (CHINARE) during 2010/2011 and 2016/2017. The zircon isotopic analyses were finished by help of Dr. Jianhui Liu and Dr. Runlong Fan at the Beijing SHRIMP Centre, Chinese Academy of Geological Sciences. This study has been financially supported by the National Nature Science Foundation of China (Grant no. 41972050). Constructive reviews and comments on the manuscript by two anonymous reviewers and Associate Editor Dr. Shi Xuefa are very much appreciated.

References

Alekseev N L, Kamennev I A, Mikhalsky E V, et al. 2021. Multistage evolution of Proterozoic crust of East Antarctica by the example of the Filla Terrane (Rauer Islands): new geological and isotope data. Rus Geol Geoph, 62(5): 557-575, doi:10.2113/RGG20194068.

Arora D, Pant N, Pandey M, et al. 2020. Insights into geological evolution of Princess Elizabeth Land, East Antarctica–clues for continental suturing and breakup since Rodinian time. Gondwana Res, 84: 260-283, doi:10.1016/j.gr.2020.05.002.

Boger S D. 2011. Antarctica–before and after Gondwana. Gondwana Res, 19(2): 335-371.

Boger S D, Wilson C J L, Fanning C M. 2001. Early Paleozoic tectonism within the East Antarctic craton: the final suture between east and west Gondwana? Geology, 29: 463-466.

Carson C J, Fanning C M, Wilson C J L. 1996. Timing of the Progress Granite, Larsemann Hills: additional evidence for Early Paleozoic orogenesis within the east Antarctic shield and implications for Gondwana assembly. Austral J Earth Sci, 43: 539-553.

Carson C J, Powell R, Wilson C J L, et al. 1997. Partial melting during

tectonic exhumation of a granulite terrane: an example from the Larsemann Hills, East Antarctica. J Metamorph Geol, 15: 105-126.

Chen L, Liu X, Wang W-RZ, et al. 2023. Ultrahigh-temperature mafic granulites in the Rauer Group, East Antarctica: evidence from conventional thermogeobarometry, phase equilibria modeling, and rare earth element thermometry. J Petrol, 64: 1-28.

Clark C, Taylor R J M, Johnson T E, et al. 2019. Testing the fidelity of thermometers at ultrahigh temperatures. J Metamorph Geol, 37: 917-934.

Dirks P H G M, Hand M. 1995. Clarifying temperature-pressure paths via structures in granulite from the Bolingen Islands, Antarctica. Austral J Earth Sci, 42: 157-172.

Dirks P H G M, Wilson C J L. 1995. Crustal evolution of the East Antarctic mobile belt in Prydz Bay: continental collision at 500 Ma? Precam Res, 75: 189-207.

Dirks P H G M, Hoek J D, Wilson C J L, et al. 1994. The Proterozoic deformation of the Vestfold Hills basement complex, East Antarctica: implications for the tectonic development of adjacent granulite belts. Precam Res, 65: 277-295.

Fitzsimons I C W. 1996. Metapelitic migmatites from Brattstrand Bluffs, East Antarctica–metamorphism, melting and exhumation of the mid-crust. J Petrol, 37: 395-414.

Fitzsimons I C W. 1997. The Brattstrand Paragneiss and the Søstrene Orthogneiss: a review of Pan-African metamorphism and Grenvillian relics in southern Prydz Bay//Ricci C A (ed). The Antarctic region: geological evolution and processes. Siena: Terra Antartica Publ, 121-130.

Fitzsimons I C W. 2000. Grenville-age basement provinces in East Antarctica: evidence for three separate collisional orogens. Geology, 28(10): 879-882.

Grew E S, Carson C J L, Christy A G, et al. 2012. New constraints from U-Pb, Lu-Hf and Sm-Nd isotopic data on the timing of sedimentation and felsic magmatism in the Larsemann Hills, Prydz Bay, East Antarctica. Precam Res, 206: 87-108.

Harley S L. 1987. Precambrian geological relationships in high-grade gneisses of the Rauer Islands, East Antarctica. Austral J Earth Sci, 34: 175-207.

Harley S L. 1988. Proterozoic granulites from the Rauer Group, East Antarctica: I. Decompression pressure-temperature paths deduced from mafic and felsic gneisses. J Petrol, 29: 1059-1095.

Harley S L. 1998. Ultrahigh temperature granulite metamorphism (1050 ℃, 12 kbar) and decompression in garnet (Mg_{70})-orthopyroxene-sillimanite gneisses from the Rauer Group, East Antarctica. J Metamorph Geol, 16: 541-562.

Harley S L. 2003. Archaean–Cambrian crustal development of East Antarctica: metamorphic characteristics and tectonic implications. Geol Soc Lond Spec Publ, 206: 203-230, doi:10.1144/GSL.SP.2003.206.01.11.

Harley S L. 2014. Antarctica in Gondwana and earlier supercontinents: evidence from the Rauer Islands region, Prydz Bay. Abstract of Chinese National Symosium on Polar Sciences, 217-218.

Harley S L. 2016. A matter of time: the importance of the duration of UHT metamorphism. J Mineral Petrol Sci, 111: 50-72.

Harley S L, Fitzsimons I C W. 1991. Pressure-temperature evolution of metapelitic granulites in a polymetamorphic terrane: the Rauer Group, East Antarctica. J Metamorph Geol, 9: 231-243.

Harley S L, Kelly N M. 2007. The impact of zircon-garnet REE distribution data on the interpretation of zircon U-Pb ages in complex high-grade terrains: an example from the Rauer Islands, East Antarctica. Chem Geol, 241: 62-87.

Harley S L, Snape I, Fitzsimons I C W. 1995. Regional correlatios and terrane assembly in East Prydz Bay: evidence from the Rauer Group and Vestfold Hills. Terra Antart, 2: 49-60.

Harley S L, Snape I, Black L P. 1998. The evolution of a layered metaigneous complex in the Rauer Group, East Antarctica: evidence for a distinct Archaean terrane. Precam Res, 89: 175-205.

Harley S L, Hokada T, Jean-Mare M, et al. 2009. Sapphirine + quartz in the Rauer Islands, Antarctica: evidence for 590 Ma UHT metamorphism. Abstract of Granulites and Granulites Conference, 1-40.

Harley S L, Fitzsimons I C W, Zhao Y. 2013. Antarctica and supercontinent evolution: historical perspectives, recent advances and unresolved issues. Geol Soc London Spec Publ, 283: 1-34.

Hensen B J, Zhou B. 1995. A Pan-African granulite facies metamorphic episode in Prydz Bay, Antarctica: evidence from Sm-Nd garnet dating, Austral J Earth Sci, 42(3): 249-258, doi:10.1080/08120099508728199.

Hensen B J, Zhou B. 1997. East Gondwana amalgamation by Pan-African collision? Evidence from Prydz Bay, East Antarctica//Ricci C A (ed). The Antarctic region: geological evolution and processes, Siena: Terra Antartica Publ, 115-119.

Hensen B J, Zhou B, Thost D E. 1995. Are reaction textures reliable guides to metamorphic histories? Timing constraints from garnet Sm-Nd chronology for ‘decompression’ textures in granulites from Søstrene Island, Prydz Bay, Antarctica. Geol J, 30(3/4): 261-271.

Hokada T, Harley S L, Dunkley D J, et al. 2016. Peak and post-peak development of UHT metamorphism at Mather Peninsula, Rauer Islands: Zircon and monazite U-Th-Pb and REE chemistry constraints. J Mineral Petrol Sci, 111(2): 89-103, doi:10.2465/JMPS.150829.

Kelsey D, Hand M, Clark C, et al. 2007. On the application of in situ monazite chemical geochronology to constraining P-T-t histories in high-temperature (>850 ℃) polymetamorphic granulites from Prydz Bay, East Antarctica. J Geol Soc Lond, 164: 667-683.

Kelsey D E, Wade B P, Collins A S, et al. 2008. Discovery of a Neoproterozoic basin in the Prydz belt in East Antarctica and its implications for Gondwana assembly and ultrahigh temperature metamorphism. Precam Res, 161(3/4): 355-388, doi:10.1016/j.precamres.2007.09.003.

Kinny P D, Black L P, Sheraton J W. 1993. Zircon ages and the distribution of Archaean and Proterozoic rocks in the Rauer Islands. Antarct Sci, 5(2): 193-206, doi:10.1017/S0954102093000252.

Liu X C. 2009. Polymetamorphism of the Prydz Belt, East Antarctica: implications for the reconstruction of the Rodinia and Gondwana supercontinents. Acta Petrol Sin, 25(8): 1808-1818 (in Chinese with English abstract).

Liu X, Zhao Y, Liu X, et al. 2002. Geology of the Grove Mountains in East Antarctica–new evidence for the final suture of Gondwana land. Sci Chin (D), 32: 457-468 (in Chinese with English abstract).

Liu X, Jahn B M, Zhao Y, et al. 2006. Late Pan-African granitoids from the Grove Mountains, East Antarctica: age, origin and tectonic implications. Precam Res, 145: 131-154.

Liu X, Zhao Y, Zhao G, et al. 2007. Petrology and geochronology of granulites from the McKaskle Hills, eastern Amery Ice Shelf, Antarctica, and implications for the evolution of the Prydz Belt. J

Petrol, 48: 1443-1470.

Liu X, Hu J, Zhao Y, et al. 2009a. Late Neoproterozoic/Cambrian high-pressure granulites from the Grove Mountains, East Antarctica: P-T-t path, collisional orogen and implications for assembly of East Gondwana. Precam Res, 174: 181-199.

Liu X, Zhao Y, Song B, et al. 2009b. SHRIMP U-Pb zircon geochronology of high-grade rocks and charnockites from the eastern Amery Ice Shelf and southwestern Prydz Bay, East Antarctica: constraints on Late Mesoproterozoic to Cambrian tectonothermal events related to supercontinent assembly. Gondwana Res, 16: 342-361.

Liu X, Zhao Y, Hu J. 2013. The c. 1000–900 Ma and c. 550–500 Ma tectonothermal events in the Prince Charles Mountains–Prydz Bay region, East Antarctica, and their relations to supercontinent evolution//Harley S L, Fitzsimons I C W, Zhao Y (eds). Antarctica and supercontinent evolution. Geol Soc London Spec Publ, 283: 95-112.

Liu X, Wang W, Zhao Y, et al. 2014. Early Neoproterozoic granulite facies metamorphism of mafic dykes from the Vestfold Block, East Antarctica. J Metamorph Geol, 32: 1041-1062.

Liu X C, Ling X X, Jahn B M. 2018. U-Th-Pb monazite and Sm-Nd dating of high-grade rocks from the Grove Mountains, East Antarctica: further evidence for a Pan-African-aged monometamorphic terrane. Adv Polar Sci, 29(2): 108-117, doi:10.13679/j.advps.2018.2.00108.

Liu X, Chen L, Wang W-RZ, et al. 2021. Deciphering early Neoproterozoic and Cambrian high-grade metamorphic events in the Archean/Mesoproterozoic Rauer Group, East Antarctica. Precam Res, 365: 106392.

Liu Z, Carvalho B B, Li W, et al. 2023. Into the high to ultrahigh temperature melting of earth's crust: investigation of melt and fluid inclusions within Mg-rich metapelitic granulites from the Mather Peninsula, East Antarctica. J Petrol, 64: 1-27.

Ludwig K R. 2001. SQUID 1.02: a user's manual. Berkeley: Berkeley Geochronological Center, Special Publication No. 2.

Ludwig K R. 2003. User's manual for Isoplot 3.00. A geochronological Toolkit for Microsoft Excel. Berkeley: Berkeley Geochronological Center, Special Publication No. 4a.

Mikhalsky E V, Alexeev N L, Kamenev I A, et al. 2019. Mafic dykes in the Rauer Islands and Vestfold Hills (East Antarctica): a chemical and Nd isotopic comparison. Precam Res, 329: 273-293, doi:10.1016/j.precamres.2018.11.014.

Mikhalsky E V, Alexeev N L, Kamenev I A, et al. 2020. Chemical composition, U-Th-Pb age, and geodynamic setting of metavolcanic Filla series (Rauer Islands, East Antarctica). Geotectonics, 54: 285-307.

Phillips G, Wilson C J L, Phillips D, et al. 2007. Thermochronological ($^{40}Ar/^{39}Ar$) evidence of early Palaeozoic basin inversion within the southern Prince Charles Mountains, East Antarctica: implications for East Gondwana. J Geol Soc London, 164: 771-784.

Ren L, Li C, Wang Y B, et al. 2016. On constraining the Pan-African high-grade metamorphism time of the Larsemann Hills, East Antarctica. Chin J Polar Sci, 28(4): 451-461 (in Chinese with English abstract).

Ren L D, Zong S, Wang Y B, et al. 2018. Distribution domains of the Pan-African event in East Antarctica and adjacent areas. Adv Polar Sci, 29(2): 87-107, doi:10.13679/j.advps.2018.2.00087.

Sheraton J W, Black L P, McCulloch M T. 1984. Regional geochemical and isotopic characteristic of high-grade metamorphic of the Prydz Bay area: the extent of Proterozoic reworking of Archaean continental crust in East Antarctica. Precam Res, 26: 169-198.

Sims J P, Wilson C J L. 1997. Strain localization and texture development in a granulite-facies shear zone-the Rauer Group, East Antarctica// Ricci C A (ed). The Antarctic region: geological evolution and processes, Siena: Terra Antartica Publ, 131-138.

Sims J P, Dirks P H G M, Carson C J, et al. 1994. The structural evolution of the Rauer Group, East Antarctica: mafic dykes as passive markers in a composite Proterozoic terrain. Antarct Sci, 6: 379-394.

Spreitzer S K, Walters J B, Cruz-Uribe A, et al. 2021. Monazite petrochronology of polymetamorphic granulite-facies rocks of the Larsemann Hills, Prydz Bay, East Antarctica. J Metamorph Geol, 39(9): 1205-1228.

Thost D E, Hensen B J, Motoyoshi Y. 1991. Two-stage decompression in garnet-bearing mafic granulites from Søstrene Island, Prydz Bay, East Antarctica. J Metamorph Geol, 9: 245-256, doi:10.1111/J.1525-1314.1991.TB00520.X.

Tingey R J. 1991. The regional geology of Archaean and Proterozoic rocks in Antarctica//Tingey R J (ed). The geology of Antarctica. Oxford: Oxford University Press, 1-73.

Tong L, Wilson C J L. 2006. Tectonothermal evolution of the ultrahigh temperature metapelites in the Rauer Group, East Antarctica. Precam Res, 149: 1-20.

Tong L, Wilson C J L, Liu X. 2002. A high-grade event of ~1100 Ma preserved within the ~500 Ma mobile belt of the Larsemann Hills, East Antarctica: further evidence from ^{40}Ar-^{39}Ar dating. Terra Antarct, 9: 73-86.

Tong L, Liu X, Wang Y, et al. 2014. Metamorphic P–T paths of metapelitic granulites from the Larsemann Hills, East Antarctica. Lithos, 192: 102-115, doi:10.1016/J.LITHOS.2014.01.013.

Tong L, Jahn B M, Liu X, et al. 2017. Ultramafic to mafic granulites from the Larsemann Hills, East Antarctica: Geochemistry and tectonic implications. J Asian Earth Sci, 145: 679-690, doi:10.1016/j.jseaes.2017.06.012.

Tong L, Liu Z, Li Z, et al. 2019. Poly-phase metamorphism of garnet-bearing mafic granulite from the Larsemann Hills, East Antarctica: P–T path, U-Pb ages and tectonic implications. Precam Res, 326: 385-398, doi:10.1016/j.precamres.2017.12.045.

Tong L, Liu Z, Wang Y. 2021. Research progress of the ultrahigh-temperature granulites in the Rauer Group, East Antarctica. J Geomechanics, 27: 705-718 (in Chinese with English abstract).

Wang Y, Tong L, Liu D. 2007. Zircon U-Pb ages from an ultra-high temperature metapelite, Rauer Group, East Antarctica: implications for overprints by Grenvillian and Pan-African events. U.S. Geological Survey, Open-File Report 2007-1047, Short Research Paper 023, doi:10.3133/of2007-1047.srp023.

Wang Y, Liu D, Chung S L, et al. 2008. SHRIMP zircon age constraints from the Larsemann Hills region, Prydz Bay, for a late Mesoproterozoic to early Neoproterozoic tectono-thermal event in East Antarctica. Am J Sci, 308(4): 573-617, doi:10.2475/04.2008.07.

Wang W, Zhao Y, Wei C, et al. 2022. High-ultrahigh temperature metamorphism in the Larsemann Hills: insights into the tectono-thermal evolution of the Prydz Bay region, East Antarctica. J Petrol, 63: 1-30.

Williams I S. 1998. U-Th-Pb geochronology by ion microprobe. Rev Econ

Geol, 7: 1-35.

Wilson C J L, Quinn C, Tong L, et al. 2007. Early Palaeozoic intracratonic shears and post-tectonic cooling in the Rauer Group, Prydz Bay, East Antarctica constrained by $^{40}Ar/^{39}Ar$ thermo-chronology. Antarct Sci, 19: 339-353.

Wu Y B, Zheng Y F. 2004. Genesis of zircon and its constraints on interpretation of U-Pb age. Chin Sci Bull, 49(15): 1554-1569, doi:10.1007/BF03184122.

Wu H B, Tong L X, Liu Z, et al. 2023. Ultrahigh-temperature metamorphism of Fe-Al-rich paragneisses in the Mather Peninsula, Rauer Group, East Antarctica: phase equilibrium modelling and zircon U-Pb ages. Act Petrol Sin, 39: 2279-2300.

Zhao Y, Liu X, Song B, et al. 1995. Constraints on stratigraphic age of metasedimentaly rocks of the Larsemann Hills, East Antarctica: possible implication for Neoproterozoic tectonics, Precam Res, 75: 175-188.

Zhao Y, Liu X H, Liu X C, et al. 2003. Pan-African events in Prydz Bay, East Antarctica, and their implications for East Gondwana tectonics. Geol Soc London Spec Publ, 206(1): 231-245, doi:10.1144/GSL.SP.2003.206.01.12.